A STRETCHING MODEL TO EXPLAIN THE SALADO BASIN (ARGENTINA)

Carolina B. CROVETTO, Iván L. NOVARA & Antonio INTROCASO

Abstract.- The Salado Basin, placed in Buenos Aires province, Argentina, is one of the most studied sedimentary basins of the area because it curiously presents a significative positive residual Bouguer anomaly. Several models were proposed to explain this gravimetric anomaly in the last 50 years. Recently, some works incorporated geoid undulations, revealing also a positive geoid anomaly over the basin. In this work, we propose a stretching model in perfect Airy isostatic balance to study the Salado Basin. We make a three-dimensional study of the basin's balance from gravity anomalies and geoid undulations, finding a strong overbalance on it.

Key-words: Salado Basin, Gravity, Geoid undulations, Stretching model.

Resumen.- *Un modelo de estiramiento para la Cuenca del Salado (Argentina)*. La cuenca del Salado, ubicada en la provincia de Buenos Aires, Argentina, es una de las cuencas sedimentarias más estudiadas del área debido a que curiosamente presenta significativos valores positivos de anomalías de Bouguer. Varios modelos han sido propuestos para explicar esta anomalía de gravedad en los últimos 50 años. Recientemente, algunos trabajos han incorporado las ondulaciones del geoide, revelando también una anomalía de geoide positiva sobre la cuenca. En este trabajo, se propone un modelo de estiramiento en perfecto equilibrio isostático de Airy para estudiar la Cuenca del Salado. Se presenta un estudio en tres dimensiones, en donde el equilibrio de la cuenca se analiza a partir de las anomalías de gravedad y ondulaciones del geoide, encontrando una fuerte sobrecompensación debajo de la misma.

Palabras clave: Cuenca del Salado, Gravedad, Ondulaciones del geoide, Modelo de estiramiento.

Carolina Beatriz Crovetto [e-mail: crovetto@fceia.unr.edu.ar]: *Grupo de Geofísica, Instituto de Física Rosario (CONICET-UNR), Pellegrini 250, 2000 Rosario, Argentina*

Iván Lionel Novara: *Grupo de Geofísica, Instituto de Física Rosario (CONICET-UNR), Pellegrini 250, 2000 Rosario, Argentina*

Antonio Introcaso: *Grupo de Geofísica, Instituto de Física Rosario (CONICET-UNR), Pellegrini 250, 2000 Rosario, Argentina*

INTRODUCTION

The Salado Basin, placed in the Buenos Aires Province, Argentina (Figure 1), has been studied for many years for its high potential as hydrocarbon's trap. This sedimentary basin is mostly placed over the continent, but it also presents a smaller part over the Argentinean continental shelf.

Twelve exploration boreholes exist over the basin, drilled by Yacimientos Petrolíferos Fiscales (YPF) and other petroleum companies. From these early explorations, the basin appears to be non-productive, but still remains sub-explored. Several seismic profiles reveal the existences of basement depths up to 7000 m in its deepest area. All the explorations over the basin are well summarized and documented in Tavella & Wright (1996).

Several models have been proposed to explain the positive residual gravity anomaly found over the Salado Basin; among them, for example Martin (1954), Orellana (1964), Introcaso (1980, 1997b). Recently, Introcaso et al. (2002) studying geoid undulations over the basin, found also a positive geoid anomaly. Earlier results, together with this new evidence, reveal the possibility of unbalance of the structure of the basin.

In the present work, we employ gravity anomalies and geoid undulations to evaluate a theoretical balanced model of the basin. We apply three-dimensional calculation to evaluate gravity anomalies and geoid undulations from this balanced model, so an important improvement is achieved respect to the previous two-dimensional works performed over the basin with gravity and geoid. Results confirm the high over-balance of the basin.

STUDIED AREA

Geological description. The Salado Basin is placed in the Buenos Aires Province, Argentina, and presents an elongated form with NW-SE inclination; it is located between 34° and 39° South Latitudes and 56° and 62° West Longitudes (Figure 1).

Following Ramos (1999) the Salado Basin is developed between Sierra de Tandilia and the Martín García Swell. Its tectonic is passive, with traction faulting gradually reaching the basin's center. This trench was shorter at the beginning, but it has grown during the Atlantic Ocean opening. It has been classified as an orthogonal pericratonic (Lesta 1974), aulacogen basin (Introcaso & Ramos 1984), with a smooth syneclise (Rolleri 1975).

The Salado basin is one of the most studied basins of the area. Twelve hydrocarbon exploration boreholes have been drilled, three of them over the continental shelf. Several studies to find water sources were also made on the basin's interior and on its borders.

Several seismic works were performed over the basin. They include the refraction studies made by YPF inland and by Lamont Geological Observatory and the Servicio de Hidrografía Naval Argentino offshore. Other exploration seismic studies have been performed by the following oil companies: Astra and Signal (inland), and Esso, Shell, Union oil and Sun Oil (offshore). More than 2,700 km of seismic lines were explored inland and 8,300 km offshore.

The basin is thus very well delimited. Its extension is estimated in 70,000 km2, 44,000 km2 inland and 26,000 km2 offshore. The sedimentary volumes are estimated in 260,000 km3, 160,000 km3 and 100,000 km3 respectively. The north, south and east limits of the Salado Basin are constituted by normal faults of several kilometers of throw, confirmed by underground data. This faulting has generated positive areas of basement blocks covered by tenths or hundred of meters of Cretaceous and Cenozoic sediments. The basement emerges for example at the Martín García Island. Two positive areas have been found; the first one, the Martín García Swell, separating the Salado Basin from the Rosario, Santa Lucía and Paraná Basins, and the second one, the Plata horst, between the Salado Basin and the Plata Este Basin. The south-east limit of the Salado Basin is also described by normal
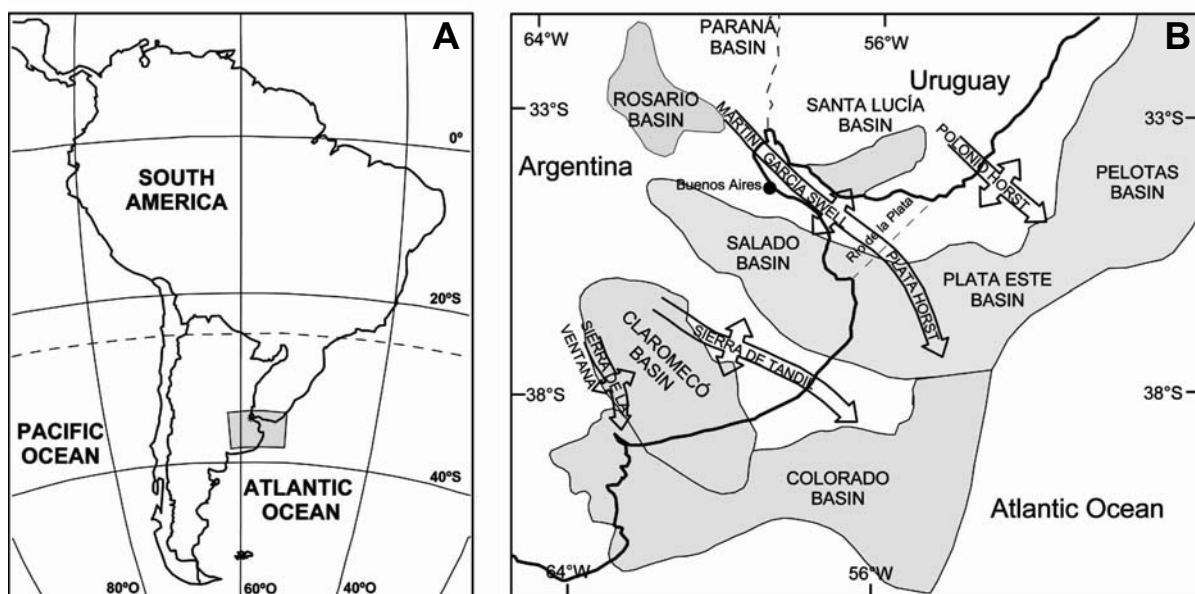

Figure 1. A: Location of the studied area in South America. **B:** Sedimentary limits of the Salado Basin and the surroundings tectonic units. Modified from Tavella & Wright (1996).

Boletín del Instituto de Fisiografía y Geología **77(1-2)**, 2007.

3

faults, with lower throws, separating the basin from the elevated basement block of the Sierras Bonaerenses. The north-west limit is the less known, but this area seems to be the one where the depositional border of the Cretaceous sequences is preserved.

Over the metamorphic Precambrian basement, similar to the that exposed in Uruguay, lower Cretaceous and upper Jurassic rocks have been found similar to those of the Paraná Basin. The maximum sedimentary thickness (mainly Cretaceous and Cenozoic) is 6500 – 7000 m. The depositional environment is mostly continental.

Previous studies. Since the first studies carried on by YPF, great attention has been paid to the Salado Basin because of the positive gravity anomaly present on it, contrary to the expected behavior for a sedimentary basin. The first gravimetric study was done by Martin (1954), who proposed that the positive gravimetric maximum observed over the basin could be attributed to an isostatic re-accommodation that did not take place during the genesis because of either the crustal rigidity or an insufficient lapse of time. Therefore, the sedimentary layers were compacted, generating the positive effect. Later, Orellana (1964) proposed the existence of an anti-root as the cause of the positive effect, while Zambrano (1974) assumed the existence of basic intrusive bodies on the bottom of the basin.

Recently, Introcaso (1980) analyzed several two-dimensional models with sedimentary layers of different densities, and concluded that the anti-root that Airy model predicts is not enough to explain the positive anomaly found. More recently, Introcaso (1997a) proposed several two-dimensional over-balanced models, with thicker anti-roots than the Airy anti-root, which together with dense basaltic materials on the bottom of the basin (compatible with materials found during the explorations), could explain the positive gravity anomalies observed inland.

Introcaso et al. (2002, 2005) employed geoid undulations to study the Salado Basin. In the first work, geoid undulations over the basin were extracted from two different sources: GPS-leveling values measured by Perdomo & Del Cogliano (1999) over the Buenos Aires province, and geoid undulations obtained from free-air gravity anomalies by the equivalent sources technique (Guspí et al. 2004). After filtering long wavelengths, residual geoid undulations from both sources show a positive anomaly of +1 m, coincident with the positive gravity anomaly found. In a preliminary isostatic analysis, geoid undulations from a balanced Airy model were computed employing one-dimensional approximations from Haxby & Turcotte (1978), finding that this balanced model could not explain the observed geoid undulations. The second work (Introcaso et al. 2005) shows several methods to obtain geoid undulations from gravity anomalies and inversely, gravity anomalies from geoid undulations, and the Salado Basin is employed as an example of application. No isostatic analysis is made in that work, but residual positive geoid undulations are also found from different methods.

Unfortunately, previous isostatic analyses made for the Salado Basin from geoid undulations lack enough precision, since one-dimensional approximations for computing geoid undulations from balanced structures have proved to be deficient in middle to short wavelengths (Crovetto et al. 2006). In view of this situation we propose in the present paper a rigorous isostatic study of the Salado Basin from geoid undulations and gravity anomalies, carrying on all the computations in three-dimensions.

OBSERVED DATA

Basement isobaths. Following Zambrano (1974), we considered as "basement" the lithostratigraphic set where the velocity is equal or more than 5 km/s. The basement isobaths corresponding to 1, 2, 3, 4, 5 and 6 km depth,
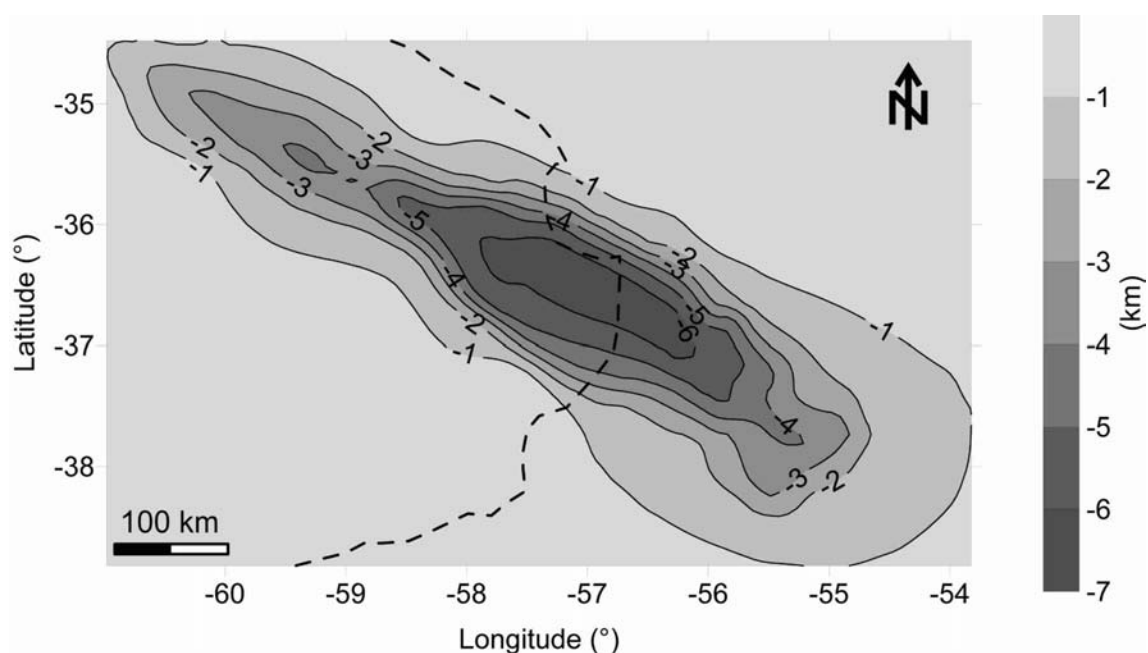

Figure 2. Basement isobaths, digitized from Zambrano (1974). The separation between contours is 1 km. The broken line shows the coast line.
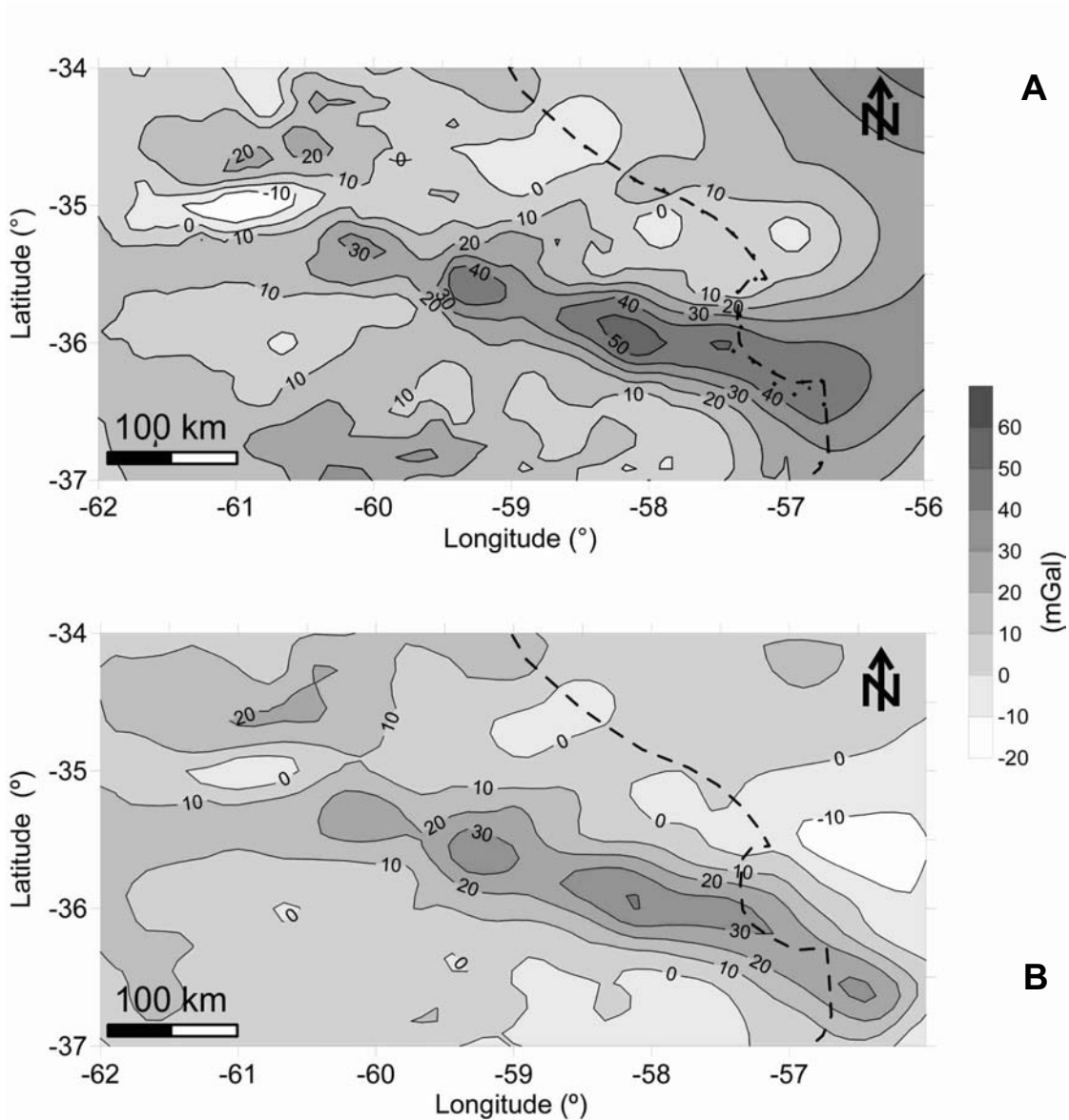
Figure 3. A: Observed Bouguer anomalies. Continental anomalies are from the IFIR database (western of 57°W), and oceanic anomalies are from Baglietto (1969) (eastern of 57°W). **B:** Residual Bouguer anomalies filtered from long and very short wavelengths. The contour separation is 10 mGal. The broken line shows the coast line.

proposed in this sense by Zambrano (1974), were digitized considering 70 points for each curve. Depths values were interpolated in order to generate a rectangular grid between 35.5 – 39° S and 54 – 61° W employing the Kriging interpolation method, with a grid spacing of 10 km x 10 km (Cressie 1991). The election of Kriging as the gridding method was done for to ensure smoothness (Figure 2).

Gravity anomalies. Observed free-air gravity anomalies were obtained from the IFIR Argentinean data base (Introcaso et al. 1996), inside a window placed between 34 – 37° S and 57 – 62° W, where the most relevant values are present. Since this data base contains only continental data, an oceanic free-air anomaly chart was employed to extend the area up to 56° W, were obtained from Baglietto (1969) through underwater gravimetric measurements performed with the remote controlled submarine "North America" and an oceanographic ship from the Servicio de Hidrografía Naval (Argentina), measuring gravity in the

bottom of the Río de la Plata and the continental shelf.

Gravity anomalies from Baglietto (1969) were digitized and joined to the IFIR anomalies. Inland Bouguer anomalies (BA) were derived from free-air anomalies (FAA) through the classical Bouguer correction:

$$BA = FAA - 2\pi G \rho_t H \qquad \textbf{(Eq. 1)}$$

where $G = 6.67 \times 10^{-8}$ cm^3/g s^2 is the universal gravitational constant, $\rho_t = 2.67$ g/cm^3 is topographic density and *H* is the topographic height (in meters), obtained from altimetry. Because of the low topography of the area, the Bouguer correction is very little and Bouguer anomalies almost coincide with free-air anomalies. Offshore Bouguer anomalies coincide with free-air anomalies.

Bouguer anomalies are shown in Figure 3A, where much contamination due to the surroundings structures (like Claromecó and Colorado Basins, and Sierras de Tandilia and Ventania) can be observed. The maximum Bouguer
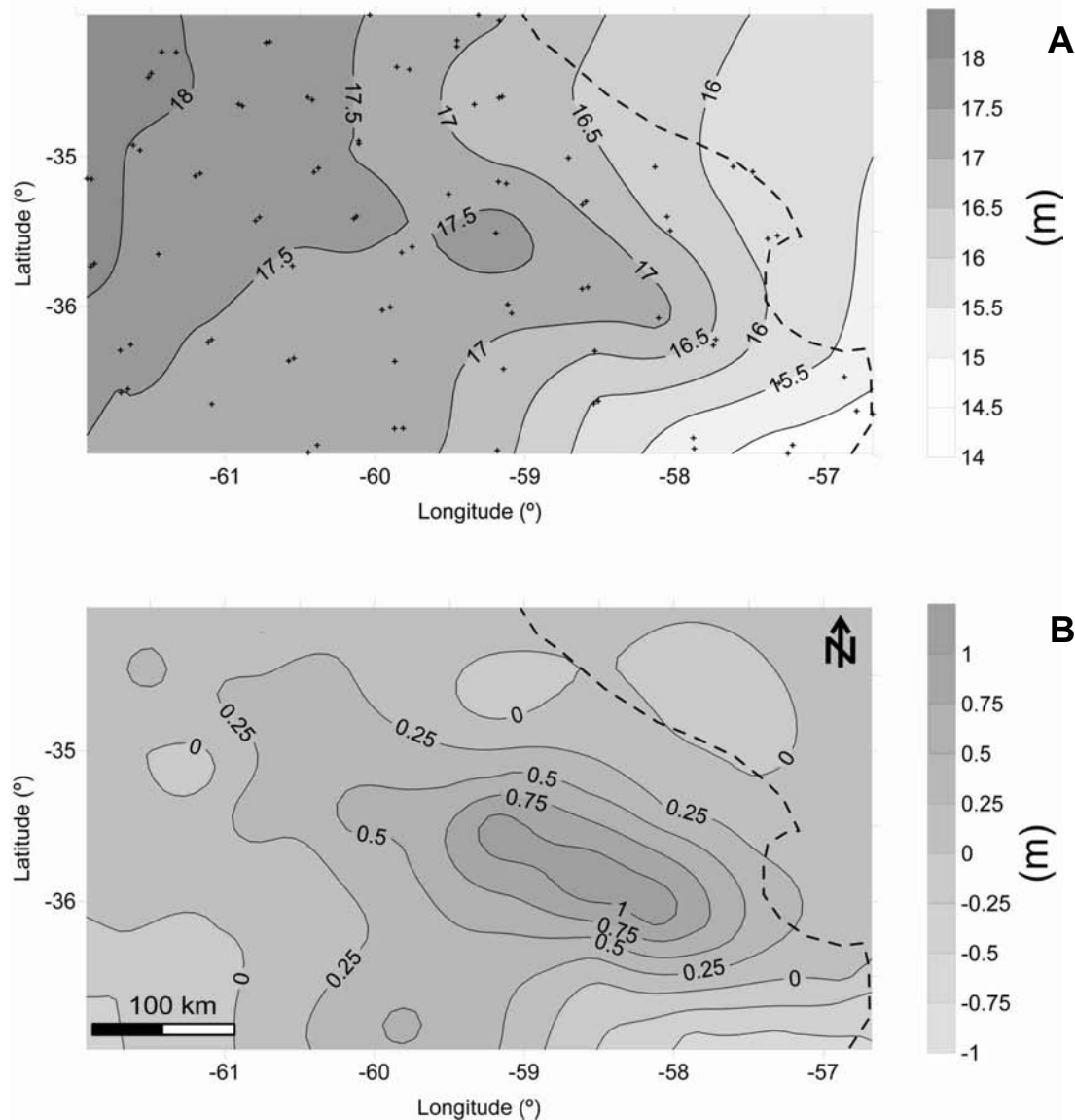
Figure 4. A: Observed geoid undulations from Perdomo & Del Cogliano (1999). Contours separation is 0.5 m. The location of the 90 *h-H* stations is shown. **B:** Residual geoid undulations. Contours separation is 0.25 m. The broken line shows the coast line.

anomaly is nearly +60 mGal, which is north-west displaced respect to the maximum depths (Figure 2).

Observed Bouguer anomalies were filtered for long and very short wavelengths to eliminate the effects of the continental masses and the surroundings structures. Several methods were evaluated to perform the filtering. The tendency surface was adopted to isolate long wavelengths (Pacino 1983), employing a plane surface of NW-SE inclination to represent the regional anomaly, coherently with Introcaso et al. (2005). Very short wavelengths were filtered through an upward continuation at 5 km, performed in the frequency domain (Guspí & Pacino, 1985). Residual Bouguer anomalies obtained after applying both filters are shown in Figure 3B.

Observed geoid undulations. Geoid undulations were taken from Perdomo & Del Cogliano (1999), who performed GPS-leveling measurements over the whole Buenos Aires Province, 90 values of *h-H* inside our study area were interpolated using again the Kriging method;

level contours are shown in Figure 4A, where the location of the original *h-H* points is also illustrated.

Observed geoid undulations were also filtered for long wavelengths employing the tendency surface method and adopting a plane surface of inclination NW-SE, coherent with regional geoid inclination for South America (Blitzkow et al. 1996). Residual geoid undulations show maximum amplitude of +1 m over the basin, similar to that found by Introcaso et al. (2002) and Introcaso et al. (2005); Figure 4B shows this residual geoid.

Sedimentary geological correction. Since geometry and density of the basin are known, a geological correction can be performed to reduce the uncertainties in the modeling procedure. This correction consists of filling of the basin with the same material as the surrounding upper crust, then remaining anomalies will show the effects of all the unknown underlying masses, different to those filling the basin. This correction can be performed over the residual
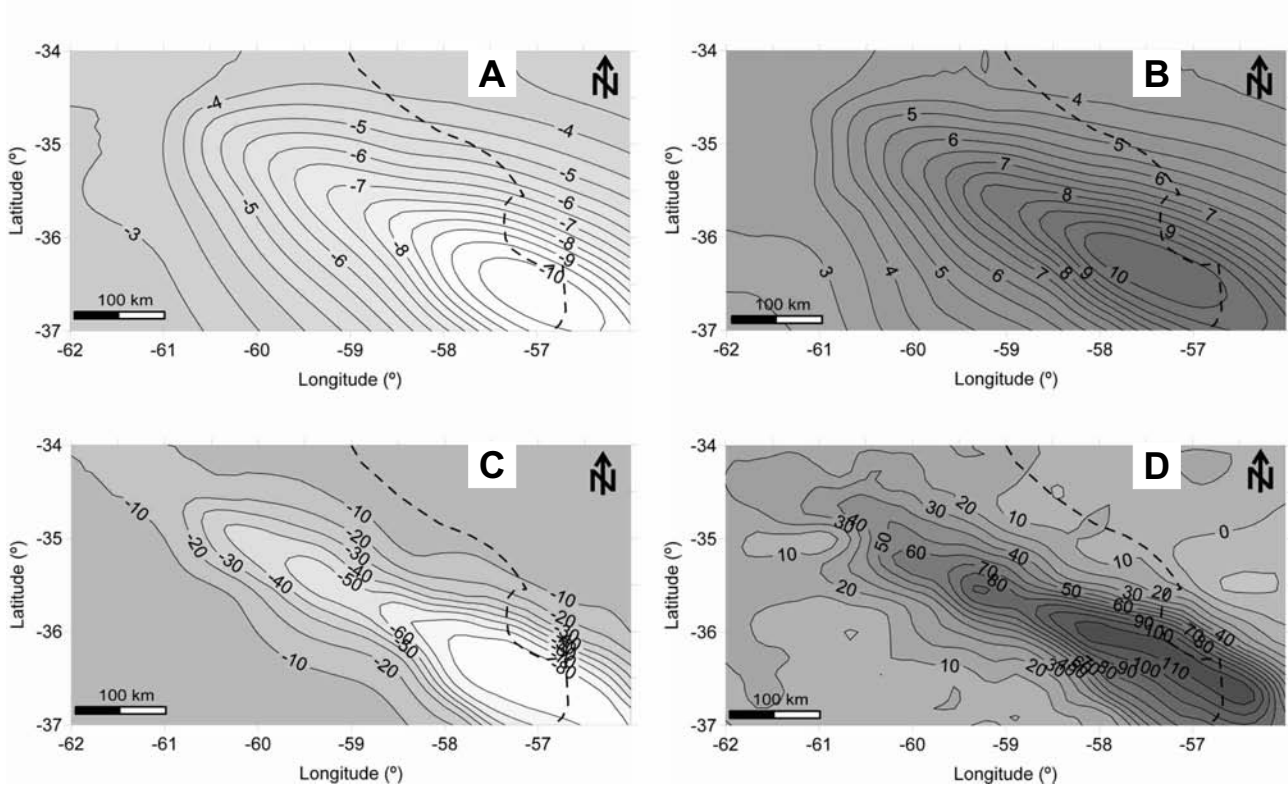
Figure 5. A: Effect of the sediments over the geoid undulations. Contours separation is 0.5 m. **B:** Geoid undulations due to the unknown underlying masses. Contours separation is 0.5 m. **C:** Effect of the sediments over the gravity anomalies. Contours separation is 10 mGal. **D:** Gravity anomalies due to the unknown underlying masses. Contours separation is 10 mGal. The broken line shows the coast line.

observed Bouguer anomalies and the residual observed geoid undulations, employing the basement isobaths (Figure 2). The corrections are opposite to the effects generated by a mass of the same shape as the basin with density equal to the difference between the sedimentary and the upper crustal densities. It can be computed decomposing the basin into a set of right rectangular prisms, of heights equal to the basin depths and density contrast $\rho_s - \rho_{uc} = (2.35 - 2.70)$ g/cm^3 = -0.35 g/cm^3, following Introcaso & Crovetto (2005); ρ_s is the density of the sediments or water filling the basin and ρ_{uc} is the upper crustal density.

For computing the gravity attraction of the prisms, the expression of Okabe (1979) was considered. Dividing the whole basin in a set of prisms, the vertical attraction of each one of them is:

$$g_z(x, y, z)$$

$$= G. \left\| \left| \left| \Delta\rho \left[x\ln(y + r) + y\ln(x + r) + 2z\arctan\frac{x + y + r}{z} \right] \right|_{x_1}^{x_2} \right|_{y_1}^{y_2} \right|_{z_1}^{z_2}$$

(Eq. 2)

where G is the universal gravitational constant, $\Delta\rho$ is the contrast density, $x_1, x_2, y_1, y_2, z_1, z_2$ are the limiting planes of the faces of the prism, $P(x, y, z)$ is the computation point, $\Delta x_i = x - x_i$, $\Delta y_i = y - y_i$, $\Delta z_i = z - z_i$, with i = 1, 2, and $r = [(\Delta x_i)^2 + (\Delta y_i)^2 + (\Delta z_i)^2]^{0.5}$ is the distance between the computation point and the vertices of the prism.

The same procedure was employed to compute the effect of the sediments on the observed geoid undulations. The gravity potential V of each prism was computed through the expression of Guspi (1999), symbols as in Equation 2:

$$V(x, y, z)$$

$$= G. \left\| \left| \left| \Delta\rho \left[xy\ln(z + r) + xz\ln(y + r) \right. \right. \right. \right.$$

$$+ yz\ln(x + r) + x^2\arctan\frac{y + z + r}{x}$$

$$\left. \left. \left. + y^2\arctan\frac{x + z + r}{y} + z^2\arctan\frac{x + y + r}{z} \right] \right|_{x_1}^{x_2} \right|_{y_1}^{y_2} \right|_{z_1}^{z_2}$$

(Eq. 3)

The Bruns' expression (Heiskanen & Moritz 1967, among others) was then employed to transform gravity potentials V of each prism into geoid undulations N of each prism:

$$N(x, y) = \frac{V(x, y, 0)}{\gamma}$$

(Eq. 4)

γ = 980 mGal normal gravity of WGS84 Model, assuming the mean latitude of the studied area.

Figure 5 shows the effects of the anomalous sedimentary mass over the geoid undulations and over the Bouguer anomalies, and the geologically corrected geoid undulations and Bouguer anomalies. The sediments
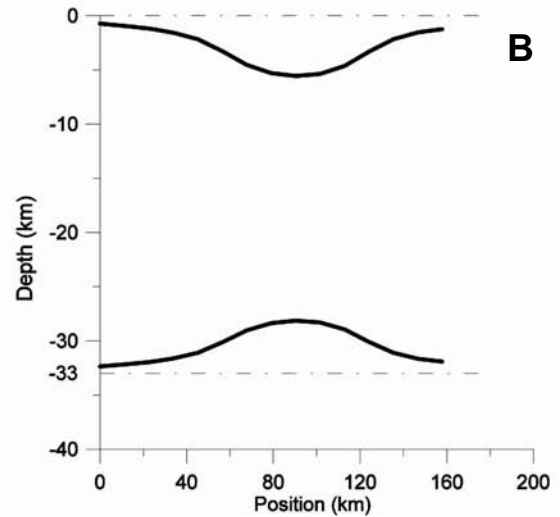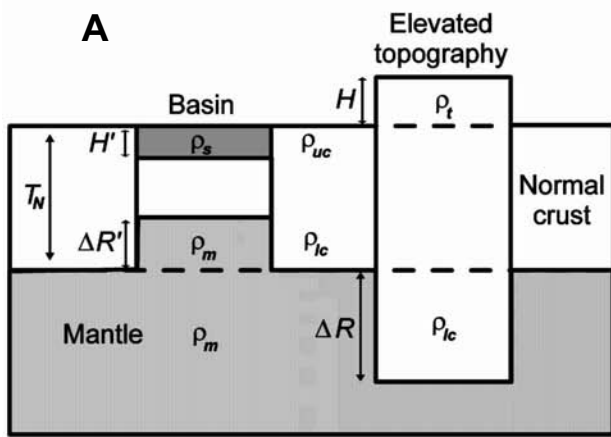
Boletín del Instituto de Fisiografía y Geología **77(1-2)**, 2007.

7

Figure 6. A: Airy's hypothesis for basins and elevated topographies. **B:** Theoretical Airy balanced model for the Salado Basin. A profile across the maximum depths is shown.

generate a negative geoid undulation of -10 m in amplitude (Figure 5A), therefore geoid undulation due to the unknown underlying masses present a positive undulation of almost 11 m in amplitude (Figure 5B). The gravity attraction of the sediments raises to -80 mGal (Figure 5C), coherently with the values found by Introcaso (1997b), computed through the least rigorous method of Talwani & Ewing (1960). The unknown underlying masses generate an attraction of more than 110 mGal in the deepest area (Figure 5D).

THEORETICAL MODEL

Airy's hypothesis. Isostasy studies the crustal equilibrium of masses. When the crust raises respect to the sea level, as in the case of a mountain, there must be some kind of mechanism that balances the mass excess due to the mountain. In the same way, in oceanic or sedimentary basins, something must equilibrate the mass defect generated by the basin filling.

Several isostatic hypotheses have been proposed, being those of Airy (1855) and Pratt (1855) the earliest ones. Both authors assume that the equilibrium is locally reached due to crustal thickness variations (Airy) or lithosphere densities variations (Pratt). Later, Vening-Meinesz (1939) proposed the flexural hypothesis, where the external layer of the lithosphere behaves as an elastic plate bending by load applications, resulting in a regional compensation system (Watts 2001).

In his hypothesis, Airy states that the crust can be divided into adjacent blocks with identical densities, floating over the mantle, in perfect hydrostatic equilibrium (Figure 6A). For reaching the equilibrium, the blocks that exceed the sea mean level present a "compensating root" which sinks into the mantle, displacing it from its position. In the case of basins, the mantle raises displacing the lower crust from its position, creating a "compensating anti-root".

Following the hydrostatic theory, the weight of any vertical anomalous column must be equal to the weight of the displaced fluid, considering the normal crust and the mantle as fluids (Introcaso, 1997a). In the case of elevated topography (Figure 6A), the compensating root of each

block must have a thickness R, then:

$$\rho_t \cdot g \cdot H \cdot A + \rho_c \cdot g \cdot T_N \cdot A + \rho_{lc} \cdot g \cdot R \cdot A$$
$$= \rho_c \cdot g \cdot T_N \cdot A + \rho_m \cdot g \cdot R \cdot A \qquad \textbf{(Eq. 5)}$$

where H is the height of the block, ρ_t is the topographic density, ρ_{lc} is the lower crustal density, ρ_c is the mean crustal density, ρ_m is the upper mantle density, T_N is the normal crustal thickness, A is the area of the section of the block, and g is mean gravity. This root is placed under the normal crustal thickness T_N, and R results:

$$R = \frac{\rho_t}{\rho_m - \rho_{lc}} H \qquad \textbf{(Eq. 6)}$$

In the case of basins, the anti-root should have a thickness R', then:

$$\rho_s \cdot g \cdot H' \cdot A + \rho_c \cdot g \cdot (T_N - H' - R') \cdot A + \rho_m \cdot g \cdot R' \cdot A$$
$$= \rho_{uc} \cdot g \cdot H' \cdot A + \rho_c \cdot g \cdot (T_N - H' - R') \cdot A + \rho_{lc} \cdot g \cdot R' \cdot A \qquad \textbf{(Eq. 7)}$$

This anti-root is placed over the normal crustal thickness T_N (Figure 6A), and R' is:

$$R' = \frac{\rho_{uc} - \rho_s}{\rho_m - \rho_{lc}} H' \qquad \textbf{(Eq. 8)}$$

In this case a stretching model is consistent with the shape of the system.

Theoretical balanced model effects. The equation (8) results $R' = 0.875H'$ where contrast-densities were assumed $\rho_s - \rho_{uc} = (2.35 - 2.70)$ g/cm^3 = - 0.35 g/cm^3 and $\rho_m - \rho_{lc} = (3.30 - 2.90)$ g/cm^3 = -0.40 g/cm^3. A profile across the maximum depths of the resulting Salado Basin balanced model is shown in Figure 6B.

The effects of this theoretical model were computed employing again the three-dimensional integration, decomposing the structure in a set of prisms.
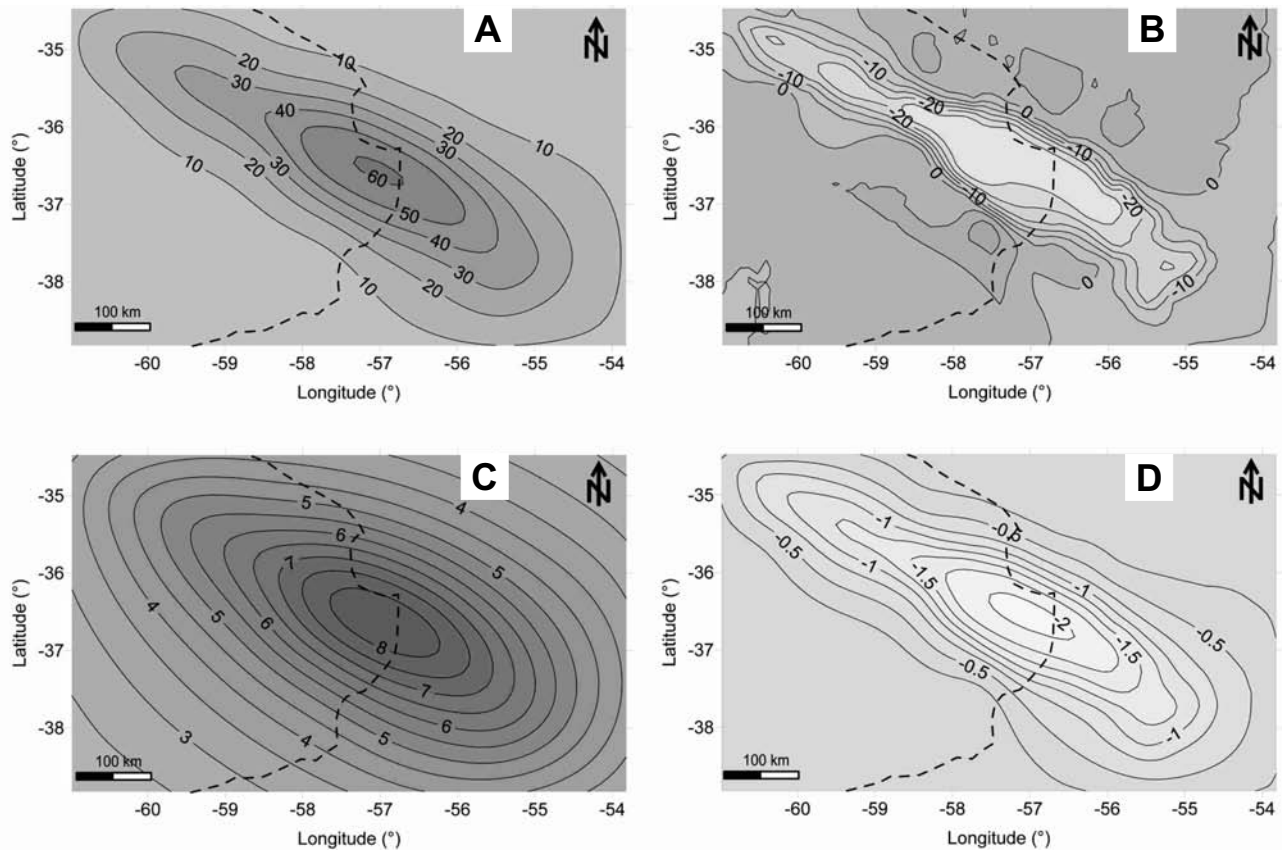
Figure 7. A: Attraction of the Airy compensating anti-root. Contour separation is 10 mGal. **B:** Theoretical Bouguer anomaly from the balanced Airy model. Contour separation is 5 mGal. **C:** Effect of the anti-root of the balanced Airy model on the geoid undulations. Contour separation is 0.5 m. **D:** Theoretical geoid undulations from the Airy balanced model. Contour separation is 0.25 m. The broken line shows the coast line.

For the basin part, the prisms were considered to have a density contrast $_s$ - $_{uc}$. For the anti-root, the prisms were considered to have a density contrast $_m$ - $_{lc}$. Equation (2) was employed for computing the gravity effect of both masses, while equations (3) and (4) were employed for computing the effects on geoid undulations. Results are shown in Figure 7, where Bouguer anomalies and geoid undulations generated by this theoretical balanced model can be appreciated. The effects of the anti-root alone are also shown, for helping in comparison.

DISCUSSION

It is clear from Figure 7, that theoretical Airy balanced model reproduces neither the observed Bouguer anomalies nor the observed geoid undulations on the Salado Basin. The Airy compensating anti-root generates lower gravity and geoid effects than the observed ones.

Gravity attraction from the compensating anti-root (Figure 7A), presents maximum amplitude of 60 mGal, while the maximum amplitude of the observed effect of the unknown underlying masses of the basin is more than 110 mGal (Figure 5D). The total Bouguer anomaly generated by this theoretical balanced model shows negative amplitude of -30 mGal over the deepest area (Figure 7B), while the observed Bouguer anomalies show positive amplitude of 30 mGal (Figure 3B).

The same behavior is present in geoid undulations. The undulations produced by the theoretical Airy compensating anti-root reach amplitude of 8 m over the deepest basin area (Figure 7C), while the undulations produced by real but unknown underlying masses is 11 m (Figure 5B). The total geoid undulations produced by this theoretical Airy balanced model show negative maximum amplitude of -2 m (Figure 7D), while the real observed total geoid undulations over the basin present a positive amplitude of 1 m (Figure 4B).

Another important feature to point out is that maximum amplitudes are displaced between actual and theoretical gravity anomalies and geoid undulations charts. Real maximum amplitudes are placed at -36°S, -58°W (Figures 3B and 4B), but theoretical maximum amplitudes are placed at -36.5°S, -57°W (Figures 7B and 7D) approximately. This difference could be attributed to the isobaths, which are responsible for the theoretical results. The employed isobaths are out of date and probably have a high degree of uncertainty that could be perturbing our results. Unfortunately, this fact did not appear in earlier works because they were all two-dimensional, considering some profiles transverse to the inland portion of the basin.

After these considerations, it becomes clear that the Salado Basin is not balanced according to Airy's hypothesis. To explain the great positive values of gravity anomalies and geoid undulations produced by the unknown underlying masses, the dimensions of those masses should exceed those proposed by Airy's hypothesis. As a result of this, the Salado Basin seems to be largely overbalanced.

Of course, the possibilities are not only limited to overbalance. Some gravimetric studies showed the necessity of considering intrusive basaltic rocks plus a strong overbalance to explain the positive Bouguer anomalies. In this sense further work is being performed to find a model that completely reproduces the observed Bouguer anomalies and the observed geoid undulations.

CONCLUSIONS

The positive Bouguer anomaly present over the Salado Basin has been the subject of several studies in the last fifty years. Employing traditional gravimetry some models were proposed to explain this positive anomalies, where an additional anti-root than that predicted by Airy's hypothesis was found to be necessary. Other models include basaltic intrusive material in the basin's bottom, coherent with some dense rocks found during explorations.

In the present paper we analyzed both, Bouguer anomalies and geoid undulations over the Salado Basin. Both charts show a positive maximum, approximately over the deepest zone of the basin. After rigorous computation of the gravity anomalies and geoid undulations produced by a balanced theoretical Airy model employing three-dimensional calculations, we realized that this model can not explain the positive values observed. An additional anti-root than that predicted by Airy, should be present under the basin to generate them. Thus, from this double interpretation of geoid and gravity, the Salado Basin seems to be overbalanced.

More complex models, including intrusive basaltic material on the bottom of the basin, are now being studied to find the model that best reproduces simultaneously the observed gravity anomalies and geoid undulations.

REFERENCES

Airy G.B., 1855. On the computation of the effect of the attraction of mountain-masses, as disturbing the apparent astronomical latitude of stations of geodetic surveys. *Philosophical Transactions of the Royal Society of London* **145**: 101-104.

Baglietto E.E., 1969. Contribuciones a la geodesia aplicada, *Instituto de Geodesia, Facultad de Ingenieria, Universidad Nacional de Buenos Aires*, 97p., Buenos Aires.

Blitzkow D., Lobianco M.C. & Fairhead J.D., 1996. Data coverage improvement for geoid computation in South America. *International Association of Geodesy Symposia, Gravity, Geoid and Marine Geodesy, International Symposium 117, Japan*: 523-531.

Cressie N.A., 1991. Statistics for Spatial Data, *John Wiley and Sons Inc.*, 900 p., New York.

Crovetto C., Molinari R. & Introcaso A., 2006.

Aproximaciones para el cálculo del geoide isostático. *Revista de la Asociación Geológica Argentina* **61(3)**: 38-48.

Guspí F., 1999. Fórmulas compactas para el cálculo del potencial gravitatorio de prismas rectangulares. *In:* Introcaso, A. *(ed.)*: *Contribuciones a la Geodesia en la Argentina de fines del siglo XX – Homenaje a Oscar Parachú, UNR Editora*: 129-133, Rosario.

Guspí F. & Pacino M.C., 1985. Prolongación ascendente y descendente de campos potenciales en el dominio frecuencial. *Geoacta* **13(1)**: 267-279.

Guspí F., Introcaso A. & Introcaso B., 2004. Gravity-enhanced representation of measured geoid undulations using equivalent sources. *Geophysical Journal International* **159**: 1-8.

Haxby W. & Turcotte D., 1978. On isostatic geoid anomalies. *Journal of Geophysical Research* **94 (B4)**: 3876-3890.

Heiskanen W. & Moritz H., 1967. Physical Geodesy. *Freeman and Company*, 364 pp., San Francisco.

Introcaso A., 1980. A gravimetric interpretation of the Salado Basin (Argentina). *Bollettino di geodesia teorica ed aplicata* **22(87)**: 187-200.

Introcaso A., 1997a. Gravimetría. *UNR Editora*, 359 pp., Rosario.

Introcaso A., 1997b. La evolución futura de la cuenca del Salado. *Tesis Doctoral Universidad Nacional de Rosario*, 150 pp., Rosario.

Introcaso A. & Ramos V., 1984. La cuenca del Salado. Un modelo de evolución aulacogénica. *Noveno Congreso Geológico Argentino (Bariloche)* **3**: 27-46.

Introcaso A., Guspí F. & Pacino M.C., 1996. Cartas gravimétricas de las anomalías de la gravedad en Argentina. *Internacional Federation of Surveyors, Symposia Papers*: 79-100.

Introcaso A., Guspí F. & Introcaso B., 2002. Interpretación del estado isostático de la Cuenca del Salado (Provincia de Buenos Aires) utilizando un geoide local obtenido mediante fuentes equivalentes a partir de anomalías de aire libre. *Actas del Decimoquinto Congreso Geológico Argentino (El Calafate). Articulo 139, 6 pp.*

Introcaso A. & Crovetto C., 2005. Introducción a la construcción del geoide, *Colección Temas de Geociencias* **12 :1-56.**

Introcaso B., Crovetto C. & Introcaso A., 2005. Obtención de una carta de g desde las ondulaciones del geoide. Aplicaciones al estudio de la cuenca del Salado (Argentina). *Tercer Congreso Cubano de Geofísica (La Habana) 23, 6 pp.*

Lesta P., 1974. Exploraciones de la patagonia continental argentina. *Comunicación Yacimientos Petrolíferos Fiscales* (Buenos Aires) **8:** 20 -41.

Martin R., 1954. Gravity Maxima corresponding with sedimentary basins. *Geophysics* **19**: 89-94.

Okabe M., 1979. Analytical expressions for gravity anomalies due to homogeneous polyhedral bodies and translations into magnetic anomalies. *Geophysics* **44(4):** 730-741.

Orellana E., 1964. Contribución al conocimiento de la corteza terrestre bajo la cuenca sedimentaria del río Salado. *Tercera Reunión Asociación Argentina de Geofísicos y Geodesias (*Rosario*)*, 53 pp.

Pacino M.C., 1983. Determinación de anomalías regionales y residuales por medio de superficies de tendencia. *Segundo Simposio Sudamericano de Cogeodata* **1**: 151-171.

Perdomo R. & Del Cogliano D., 1999. The geoid in Buenos Aires region. *International Geoid Service, Bulletin, Special Issue for South America* **9**: 109-116.

Pratt J.H., 1855. On the attraction of the Himalaya Mountains, and of the elevated regions beyond them, upon the plumb line in India. *Philosophical Transactions of The Royal Society of London* **145**: 53-100.

Ramos V., 1999. Las provincias geológicas del territorio argentino. *In:* R. Caminos *(ed.)*: Geología Argentina. *Anales del Servicio Geológico y Minero Argentino* **29 (3)**: 41-93.

Rolleri E., 1975. Provincias geologicas bonaerenses. *In:* Geología de la Provincia de Buenos Aires. *Relatorio del Sexto Congreso Geologico Argentino (Buenos Aires)*: 29-53.

Talwani M. & Ewing M., 1960. Rapid computation of gravitational attraction of three-dimensional bodies of arbitrary shape. *Geophysics* **25**: 203-225.

Tavella G. & Wright C., 1996. Cuenca del Salado. *Decimotercero Congreso Geológico Argentino y Tercer Congreso de Exploración de Hidrocarburo, Buenos Aires. In*: V.A.Ramos y M.A.Turic *(ed.)*: Geología y Recursos Naturales de la Plataforma Continental Argentina, Relatorio* **6**: 95-116.

Vening-Meinesz F.A., 1939. Tables foundamentales pour la réduction isostatique régionale. *Bulletin Géodésique* **63**: 711-776.

Watts A.B., 2001. Isostasy and flexure of the lithosphere. *Cambridge University Press,* 458 pp., Cambridge.

Zambrano J.J., 1974. Cuencas Sedimentarias en el subsuelo de la provincia de Buenos Aires y zonas adyacentes. *Revista de la Asociación Geológica Argentina* **29(4)**: 443-449.